APPENDIX A

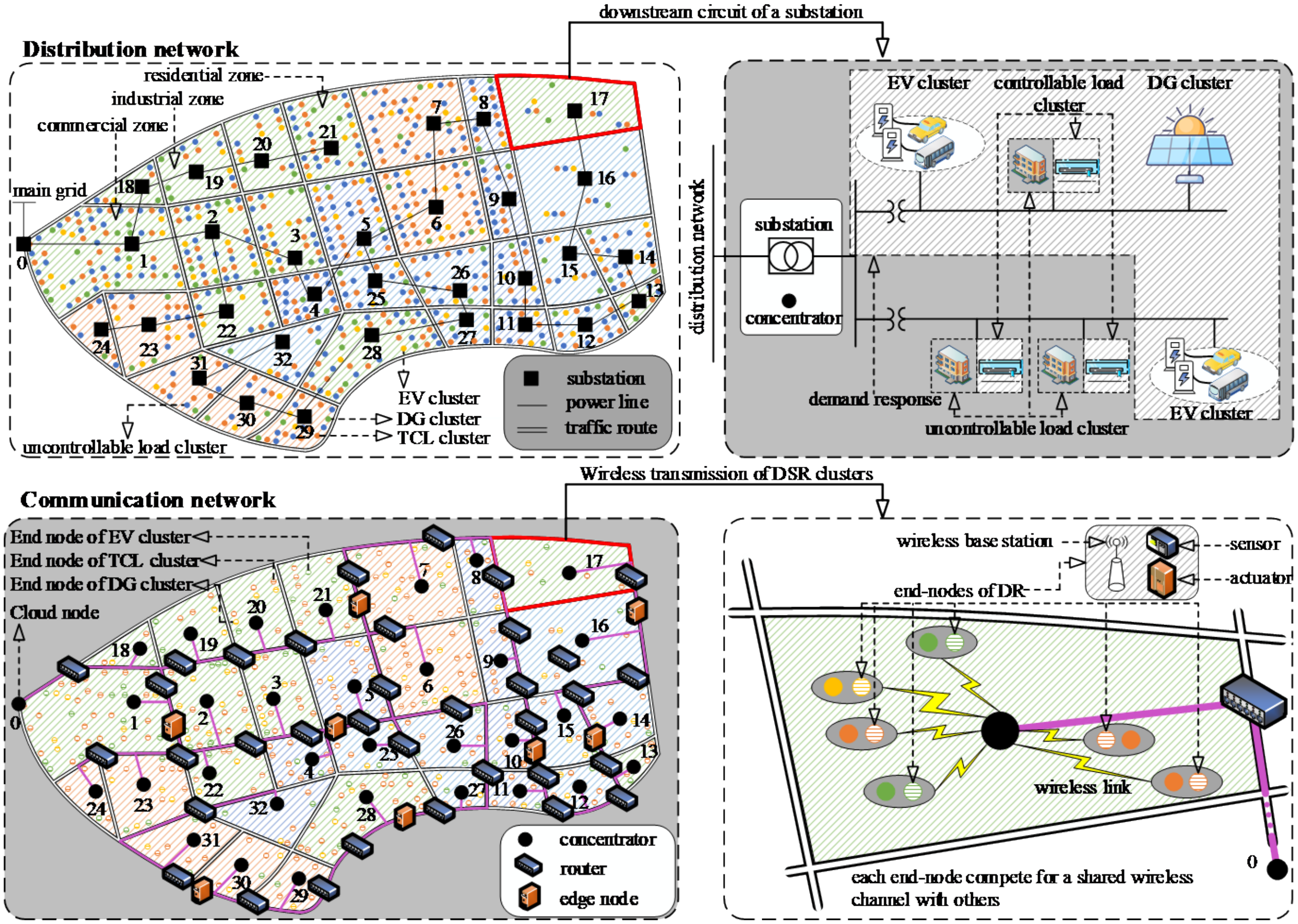

Fig.A1 Smart distribution network consisting of a distribution network and corresponding communication network.

APPENDIX B

A. AC Power Flow Model Based on SOCP

Three consecutive substations s_1, s_2 and s_3 of a radial distribution network are illustrated in Fig. B1. Where the complex power of power line (s_1,s_2) and substation s_1 are expressed by $P_t(s_1,s_2)+\mathrm{i}Q_t(s_1,s_2)$ and $P_t(s_1)+\mathrm{i}Q_t(s_1)$ at time t. Let $I_t(s_1,s_2)$ and $V_t(s_1)$ be the current flow of power line (s_1,s_2) and voltage of substation s_1 at the scheduling time t, respectively. The resistance and reactance of power line (s_1,s_2) are denoted by $r(s_1,s_2)$ and $x(s_1,s_2)$. Thus, equations of power flow are as follows:

$$P_t(s_2,s_3)=P_t(s_1,s_2)-\frac{P_t(s_1,s_2)^2+Q_t(s_1,s_2)^2}{V_t(s_1)^2}r(s_1,s_2)-P_t(s_2) \tag{B1}$$

$$Q_t(s_2,s_3)=Q_t(s_1,s_2)-\frac{P_t(s_1,s_2)^2+Q_t(s_1,s_2)^2}{V_t(s_1)^2}x(s_1,s_2)-Q_t(s_2) \tag{B2}$$

$$I_t(s_1,s_2)^2=\frac{P_t(s_1,s_2)^2+Q_t(s_1,s_2)^2}{V_t(s_1)^2} \tag{B3}$$

$$\begin{aligned}V_t(s_2)^2&=V_t(s_1)^2-2\big(r(s_1,s_2)P_t(s_1,s_2)+x(s_1,s_2)Q_t(s_1,s_2)\big)\\&+\big(r(s_1,s_2)^2+x(s_1,s_2)^2\big)\frac{P_t(s_1,s_2)^2+Q_t(s_1,s_2)^2}{V_t(s_1)^2}\end{aligned} \tag{B4}$$

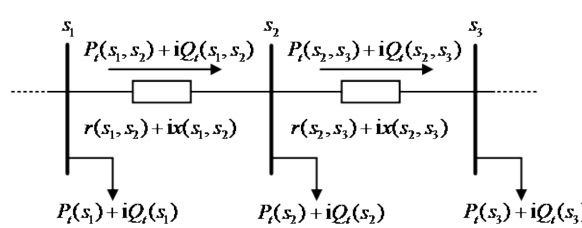

Fig.B1 Equivalent model of radial distribution network at scheduling time t.

For above nonlinear equations, second-order cone programming is applied to transform the calculation of power flow into a convex programming problem [32]. Besides, the quadratic components of $I_t(s_1,s_2)$ and $V_t(s_1)$ are replaced with $V_{q,t}(s_1)$ and $I_{q,t}(s_1,s_2)$ to linearize these equations. Then, modified AC power flow model is shown as:

$$\left\|\begin{matrix}2P_t(s_1,s_2)\\2Q_t(s_1,s_2)\\I_{q,t}(s_1,s_2)-V_{q,t}(s_1)\end{matrix}\right\|_2\le I_{q,t}(s_1,s_2)+V_{q,t}(s_1) \tag{B5}$$

$$P_t(s_2,s_3)=P_t(s_1,s_2)-I_{q,t}(s_1,s_2)r(s_1,s_2)-P_t(s_2) \quad \text{(B6)}$$

$$Q_t(s_2,s_3)=Q_t(s_1,s_2)-I_{q,t}(s_1,s_2)x(s_1,s_2)-Q_t(s_2) \quad \text{(B7)}$$

$$\begin{aligned} V_{q,t}(s_2)=&V_{q,t}(s_1)-2\left(r(s_1,s_2)P_t(s_1,s_2)+x(s_1,s_2)Q_t(s_1,s_2)\right)\\ &+\left(r(s_1,s_2)^2+x(s_1,s_2)^2\right)I_{q,t}(s_1,s_2) \end{aligned} \quad \text{(B8)}$$

To maintain the operational security of system, the voltage and current should meet the following constraints:

$$V_{\min}^2(s)\le V_{q,t}(s)\le V_{\max}^2(s) \quad \forall s\in S \quad \text{(B9)}$$

$$I_{\min}^2(s_1,s_2)\le I_{q,t}(s_1,s_2)\le I_{\max}^2(s_1,s_2) \quad \forall (s_1,s_2)\in E_p \quad \text{(B10)}$$

where $V_{\min}(s)$ and $V_{\max}(s)$ represent the maximum and minimum voltage of substation, $I_{\min}(s_1,s_2)$ and $I_{\max}(s_1,s_2)$ are the maximum and minimum current flow of power line.

From the view of power balance, $P_t(s)$ and $Q_t(s)$ equals to the total active and reactive power of clusters belonging to power supply district s. We define $P_{(\cdot),t}(j)$ as the active power of different types of DSR cluster. Then, $P_t(s)$ is constrained to the active power balance:

$$\begin{aligned} P_t(s)=&\sum_{j\in N_{\mathrm{UL}}(s)}P_{\mathrm{UL},t}(j)+\sum_{j\in N_{\mathrm{TCL}}(s)}P_{\mathrm{TCL},t}(j)+\sum_{j\in N_{\mathrm{EV}}(s)}P_{\mathrm{EV},t}(j)\\ &+\sum_{j\in N_{\mathrm{DPV}}(s)}P_{\mathrm{DPV},t}(j)+\sum_{j\in N_{\mathrm{DWP}}(s)}P_{\mathrm{DWP},t}(j)+\sum_{j\in N_{\mathrm{DES}}(s)}P_{\mathrm{DES},t}(j) \end{aligned} \quad \text{(B11)}$$

With reference to [39], TCL cluster, DPV cluster and DWP cluster are considered to operate with constant power factor, so that their active power can be scheduled independently. The remaining types of DSR clusters have no contribution to the reactive power of district. As such, $Q_t(s)$ is constrained to the reactive power balance:

$$\begin{aligned} Q_t(s)=&\sum_{j\in N_{\mathrm{UL}}(s)}Q_{\mathrm{UL},t}(j)+\sum_{j\in N_{\mathrm{TCL}}(s)}Q_{\mathrm{TCL},t}(j)+\sum_{j\in N_{\mathrm{DPV}}(s)}Q_{\mathrm{DPV},t}(j)\\ &+\sum_{j\in N_{\mathrm{DWP}}(s)}Q_{\mathrm{DWP},t}(j)+Q_{\mathrm{SVG},t}(s) \end{aligned} \quad \text{(B12)}$$

$$\begin{cases} Q_{\mathrm{TCL},t}(j)=P_{\mathrm{TCL},t}(j)\tan\varphi_{\mathrm{TCL}}(j) & \forall j\in\bigcup_{s\in S}N_{\mathrm{TCL}}(s)\\ Q_{\mathrm{DPV},t}(j)=P_{\mathrm{DPV},t}(j)\tan\varphi_{\mathrm{DPV}}(j) & \forall j\in\bigcup_{s\in S}N_{\mathrm{DPV}}(s)\\ Q_{\mathrm{DWP},t}(j)=P_{\mathrm{DWP},t}(j)\tan\varphi_{\mathrm{DWP}}(j) & \forall j\in\bigcup_{s\in S}N_{\mathrm{DWP}}(s) \end{cases} \quad \text{(B13)}$$

where $Q_{\mathrm{SVG},t}(s)$ is the reactive power of SVG, $\varphi_{\mathrm{TCL}}(j)$, $\varphi_{\mathrm{DPV}}(j)$ and $\varphi_{\mathrm{DWP}}(j)$ represent the power factor angle of TCL cluster, DPV cluster and DWP cluster.

B. Wired and Wireless Transmission Model

Assume that each power supply district is assigned only one wireless channel for communication, and each end node also needs to delivery only one data packet during the scheduling period. Within a power supply district, the wireless upload delay of each end node is generated by its competition with other end nodes for the shared wireless channel based on slotted Aloha medium access control (MAC) protocol [33]-[34]. At the beginning of a time slot, each end node should delivery its data packet with same packet size to respective concentrator with probability α. To keep stability of wireless transmission, the probability is set as $\alpha=1/n_{\mathrm{all}}(s)$, where $n_{\mathrm{all}}(s)$ is the number of clusters within power supply district $s\in S\backslash 0$. If the packet of an end node is delivered, and other end nodes within the same district do not deliver their packets at the same time, the packet will be successfully accepted by the concentrator. Otherwise, the packet will be continuously redelivered in the following time slots until it succeeds. As such, we can derive the average wireless upload delay $\overline{D}_{\mathrm{wl,up}}(s)$ of power supply district $s\in S\backslash 0$:

$$\begin{cases} \sigma_{\mathrm{s}}(q)=\alpha(1-\alpha)^{q-1}\\ W_X(x\mid q)=\sigma_{\mathrm{s}}(q)(1-\sigma_{\mathrm{s}}(q))^{x-1}\\ \overline{D}_{\mathrm{wl,up}}(s)=\sum_{q=1}^{n_{\mathrm{all}}}\sum_{x=1}^{\infty}xW_X(x\mid q)T=\sum_{q=1}^{n_{\mathrm{all}}}\dfrac{T}{\sigma_{\mathrm{s}}(q)}\\ n_{\mathrm{all}}(s)=\sum\left|N_{(\cdot)}(s)\right| \end{cases} \quad \text{(B14)}$$

where $\sigma_{\mathrm{s}}(q)$ and $W_X(x|q)$ are the probability of successful packet delivery and the probability mass function of the quantity of delivery attempts X required for successful packet delivery, respectively, when the quantity of undelivered data packet is q. T is the time slot for delivering one data packet.

During the download process, each concentrator occupies its single wireless channel to deliver scheduling instructions of clusters based on a certain wireless download queue. The cluster with greater scheduled flexibility has a higher order in the queue. Besides, since the packet size of instruction is much smaller than the operation data, the duration for wireless download also takes the minimum indivisible period T. Thus, the wireless download delay of DSR cluster j can be obtained as (B15), where $n_{\mathrm{dw},t}(j)$ is the download order of instruction.

$$D_{\mathrm{wl,dw},t}(j)=n_{\mathrm{dw},t}(j)\cdot T \quad \text{(B15)}$$

The wired delay is generated by transmitting data packet between cloud/edge nodes and concentrators, which can be calculated as [35].

$$D_{\mathrm{w}}\left[\pi(i,j)\right]=\sum_{(a,b)\in\pi(i,j)}\frac{\varphi(i)}{r(a,b)}+\sum_{(a,b)\in\pi(i,j)}\frac{d(a,b)}{v(a,b)}+\sum_{a\in\pi(i,j)}E[T_{\mathrm{br}}(a)] \quad \text{(B16)}$$

In (B16), the first term is the serial delay that equals to the fraction the data size $\varphi(i)$ of packet delivered from node i over link rate $r(a,b)$. The second term is the propagation delay that depends on the fraction the distance $d(a,b)$ over the propagation speed $v(a,b)$. The last term is the expected service delay $T_{\mathrm{br}}(a)$ of communication nodes within the wired path. In this paper, each link has enough bandwidth for data transmission, which means the communication congestion does not exist. Thus, the wired path between any two nodes can be determined by using Dijkstra algorithm for the minimum wired delay. The weight of link depends on the sum of its propagation delay and expected service delay of both ends of link.

C. Preparations for Formulation of Offloading Strategy

Before formulating the offloading strategy of both stages, the calculation delay of edge computation should be analyzed quantitatively. For the edge node $e\in E$, the calculation power is defined as $\delta(e)$, whereas $\omega(e)$ represents the queue for storing the serial number of edge calculations waiting for being processed. The serial number of edge calculations is equivalent to the number of corresponding districts $s\in S\backslash 0$. In the queue $\omega(e)$, the serial number of edge calculations is ranked from low to high based on their arrival time $t_a(s)$. Moreover, each edge calculation will not be processed until all edge calculations with lower order have been finished in $\omega(e)$. Based on the above conditions, the starting time $t_s(s)$ of edge computation in the queue $\omega(e)$ is given as:

$$t_{\mathrm{s}}[\omega_k(e)] = \begin{cases} \max\left\{t_{\mathrm{a}}[\omega_k(e)], t_{\mathrm{s}}[\omega_{k-1}(e)] + D_{\mathrm{c}}[\omega_{k-1}(e)]\right\} & k \neq 1 \\ t_{\mathrm{a}}[\omega_k(e)] & k = 1 \end{cases} \tag{B17}$$

where $\omega_k(e)$ and $\omega_{k-1}(e)$ represent the k-th and k-1th position of queue $\omega(e)$, respectively. $D_c[\omega_{k-1}(e)]$ is the computation delay of edge computation $\omega_{k-1}(e)$, which equals to the sum of waiting duration and calculation duration.

$$D_{\mathrm{c}}[\omega_{k-1}(e)] = t_{\mathrm{s}}[\omega_{k-1}(e)] - t_{\mathrm{a}}[\omega_{k-1}(e)] + \frac{\varepsilon[\omega_{k-1}(e)]}{\delta(e)} \tag{B18}$$

In (B18), $\varepsilon[\omega_{k-1}(e)]$ represents the number of CPU cycles required for the edge computation $\omega_{k-1}(e)$.

APPENDIX C

A. Maximum Schedulable Flexibility of EV Cluster

At each scheduling time, the end node of EV cluster needs to upload the operational data of EVs parked in the cluster to the concentrator. We define the operational data of EV as the set $Z_{\mathrm{EV},t}(i)=\{U_{\mathrm{EV}}(i), \xi_{\mathrm{EV}}(i), E_{\min}(i), E_{\mathrm{EV},t}(i), m_{\mathrm{p},t}(i)\}$. In the above set, $U_{\mathrm{EV}}(i)$ is the storage capacity, $\xi_{\mathrm{EV}}(i)$ is the charging and discharging efficiency, $E_{\min}(i)$ is the lower limit of state of charge (SOC) that is set for the travel demand of EV owner, $E_{\mathrm{EV},t}(i)$ is the SOC of EV, and $m_{\mathrm{p},t}(i)$ is the serial number of EV cluster where EV is parked. If EV is on driving state during the scheduling period [t, t+1], $m_{\mathrm{p},t}(i)$ equals to the value 0. Then, the maximum schedulable upward flexibility and downward flexibility of EV cluster ($F^{+}_{\mathrm{EV,max},t}(j)$ and $F^{-}_{\mathrm{EV,max},t}(j)$) can be obtained as:

$$F^{+}_{\mathrm{EV,max},t}(j) = \sum_{i\in\{k|m_{\mathrm{p},t}(k)=j\}} \max\left\{0, \min\left\{\begin{matrix} P_{\max}(m_{\mathrm{p},t}(i)), \\ \dfrac{-P_{\max}(m_{\mathrm{p},t}(i))\xi_{\mathrm{EV}}(i)}{\Delta t/\Delta t_{\mathrm{remain}}} \end{matrix}\right\}\right\} \tag{C1}$$

$$\begin{aligned} F^{-}_{\mathrm{EV,max},t}(j) = & \sum_{i\in\left\{k\left|\begin{smallmatrix} m_{\mathrm{p},t}(k)=j\cup \\ E_{\mathrm{EV},t}(k)\geq E_{\min}(k)\end{smallmatrix}\right.\right\}} \min\left\{\begin{matrix} P_{\max}(m_{\mathrm{p},t}(i)), \\ \dfrac{\left(1-E_{\mathrm{EV},t}(i)\right)U_{\mathrm{EV}}(i)}{\xi_{\mathrm{EV}}(i)\Delta t} \end{matrix}\right\} \\ & + \sum_{i\in\left\{k\left|\begin{smallmatrix} m_{\mathrm{p},t}(k)=j\cup\Delta t_{\mathrm{remain}}<\Delta t \\ \cup E_{\mathrm{EV},t}(k)<E_{\min}(k)\end{smallmatrix}\right.\right\}} \min\left\{\begin{matrix} P_{\max}(m_{\mathrm{p},t}(i)), \\ \dfrac{\left(1-E_{\min}(i)\right)U_{\mathrm{EV}}(i)}{\left(\Delta t-\Delta t_{\mathrm{remain}}\right)\xi_{\mathrm{EV}}(i)} \end{matrix}\right\} \end{aligned} \tag{C2}$$

$$\Delta t_{\mathrm{remain}} = \frac{\left(E_{\min}(i) - E_{\mathrm{EV},t}(i)\right)U_{\mathrm{EV}}(i)}{P_{\max}(m_{\mathrm{p},t}(i))} \tag{C3}$$

where $\Delta t_{\mathrm{remain}}$ is the remaining duration of EVs with $E_{\mathrm{EV},t}(j)< E_{\min}(j)$ for scheduling their downward flexibility, Δt is the scheduling period. Note that the schedulable flexibility of EV cannot be higher than the charging/discharging power of EV cluster, i.e., $P_{\max}(j)$. Besides, these EVs with $E_{\mathrm{EV},t}(j)<E_{\min}(j)$ cannot supply the upward flexibility, and can supply the downward flexibility only when their SOC satisfy $E_{\mathrm{EV},t}(j)> E_{\min}(j)$ within the scheduling period [t, t+1]. If the EV cluster is scheduled to supply the upward/downward flexibility ($F^{+}_{\mathrm{EV},t}(j)$ or $F^{-}_{\mathrm{EV},t}(j)$), its active power will be changed into:

$$P_{\mathrm{EV},t}(j) = P_{\mathrm{EV,in},t}(j) + F^{-}_{\mathrm{EV},t}(j) - F^{+}_{\mathrm{EV},t}(j) \tag{C4}$$

$$P_{\mathrm{EV,in},t}(j) = \sum_{i\in\left\{k\left|\begin{smallmatrix} m_{\mathrm{p},t}(k)=j\cup \\ E_{\mathrm{EV},t}(k)<E_{\min}(k)\end{smallmatrix}\right.\right\}} \min\left[\begin{matrix} \dfrac{\left(E_{\min}(i)-E_{\mathrm{EV},t}(i)\right)U_{\mathrm{EV}}(i)}{\Delta t}, \\ P_{\max}(m_{\mathrm{p},t}(i)) \end{matrix}\right] \tag{C5}$$

where $P_{\mathrm{EV,in},t}(j)$ represents the active load of EV cluster.

B. Maximum Schedulable Flexibility of TCL Cluster

The single-order thermal parameters of an air-conditioner are introduced as [35]:

$$C(i)\frac{\mathrm{d}\theta_{\mathrm{in},t+\tau}(i)}{\mathrm{d}\tau} = \frac{\theta_{\mathrm{out},t}(i) - \theta_{\mathrm{in},t+\tau}(i)}{R(i)} - \eta(i)P_{\mathrm{TCL},t+\tau}(i) \tag{C6}$$

$$P_{\mathrm{TCL},t+\tau}(i) = \begin{cases} 0 & \theta_{\mathrm{in}}(t+\tau;i) < \theta_t^{-}(i) \\ P_{\mathrm{TCL,N}}(i) & \theta_{\mathrm{in}}(t+\tau;i) > \theta_t^{+}(i) \\ P_{\mathrm{TCL},t+\tau-\Delta\tau}(i) & \text{otherwise} \end{cases} \tag{C7}$$

In (C6), $C(i)$ and $R(i)$ are the equivalent heat capacity and thermal resistance, $\theta_{\mathrm{in},t+\tau}(i)$ and $\theta_{\mathrm{out},t}(i)$ are the real-time indoor temperature at time t+τ and the outdoor temperature at time t. $P_{\mathrm{TCL},t+\tau}(i)$ takes the value of the rated power $P_{\mathrm{TCL,N}}(i)$ if it is on cooling state, and takes the value 0 if it is on standby state. In (C7), $\theta_t^{+}(i)$ and $\theta_t^{-}(i)$ are the upper and lower limit for the transition of air-conditioner states, which corresponds to the cooling and standby state. $\Delta\tau$ is a small time-lag approaching to value 0.

The operational data of air-conditioner for is given as $Z_{\mathrm{TCL},t}(i)$ $=\{R(i), C(i), \eta(i), P_{\mathrm{TCL,N}}(i), m_{\mathrm{c}}(i), \theta_t^{+}(i), \theta_t^{-}(i), \theta_{\mathrm{out},t}(i), \theta_{\mathrm{in},t}(i), r_t(i), y_t(i)\}$. In the above set, $m_c(i)$ is the serial number of TCL cluster that the air-conditioner belongs to, $r_t(i)$ is a status variable for judging whether the air-conditioner is schedulable or not at the scheduling time t, which takes 1 if it is schedulable, otherwise takes 0, $y_t(i)$ is the operation state of non-scheduled air-conditioner, which takes value 0/1 if TCL is on standby / cooling state, and takes value -1 if it cannot be scheduled by the operator. Only when the air-conditioner is on cooling/standby state, it is considered as the schedulable one.

According to the discussion on TCL, the value of $\theta_{\mathrm{in},t+\tau}(i)$ varies periodically within the range [$\theta_t^{+}(i)$, $\theta_t^{-}(i)$], when TCL is not scheduled. If the TCL is scheduled, the curve of indoor temperature within period [t, t+1] will be altered. We call the above two conditions of air-conditioner the proper operation mode and the scheduled mode. Fig. C1 shows the figure corresponding to the different initial indoor temperature range. $\theta^{+}_{\mathrm{user},t}(i)$/$\theta^{-}_{\mathrm{user},t}(i)$ are the upper/lower limit of indoor temperature when TCL is on the scheduled mode, as given in (C8) for users' comfortability:

$$\begin{cases} \theta^{+}_{\mathrm{user},t}(i) = (1+\mu\%)\theta_t^{+}(i) \\ \theta^{+}_{\mathrm{user}t}(i) = (1-\mu\%)\theta_t^{-}(i) \end{cases} \tag{C8}$$

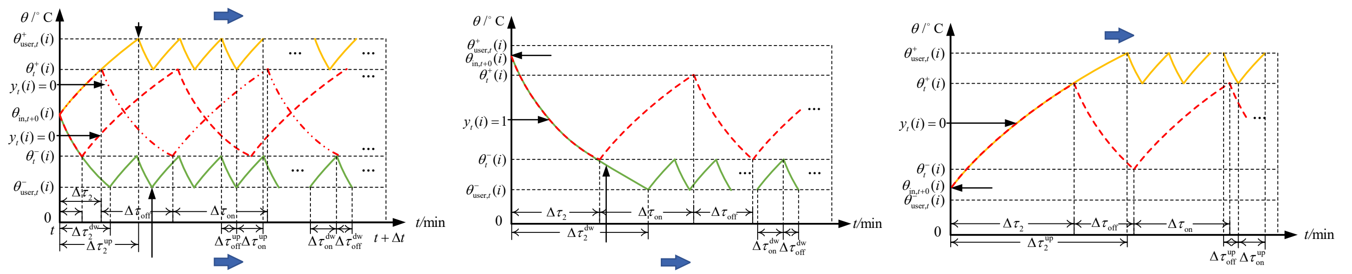

(a) $\theta_t^-(i)<\theta_{\text{in},t+0}(i)<\theta_t^+(i)$ (b) $\theta_{\text{in},t+0}(i)\geq\theta_t^+(i)$ (c) $\theta_{\text{in},t+0}(i)\leq\theta_t^-(i)$

Fig.C1 Indoor temperature curve of air-conditioner with $r_t(i)$=1 under different conditions of initial indoor temperature $\theta_{\text{in},t+0}(i)$

where μ% is the sliding scales of temperature limit. If $\theta_{\text{in},t+\tau}(i)\geq\theta^+_{\text{user},t}(i)$, the state of air-conditioner will be forced into cooling state until $\theta_{\text{in},t+\tau}(i)\leq\theta_t^+(i)$. In the same way, if $\theta_{\text{in},t+\tau}(i)\leq\theta^-_{\text{user},t}(i)$, the state of air-conditioner will be forced into standby state until $\theta_{\text{in},t+\tau}(i)\geq\theta_t^-(i)$. Since the state of TCL cannot be altered frequently, the air-conditioner can be scheduled to supply upward or downward flexibility if its indoor temperature meets the range $\theta_{\text{in},t+\tau}(i)\in(\theta^-_{\text{user},t}(i),\theta_t^+(i))$ or $(\theta_t^-(i),\theta^+_{\text{user},t}(i))$.

For clear understanding, we take Fig.C1 (a) as an example to derive the formula for flexibility calculation. In Fig. C1 (a), the value of $\theta_{\text{in},t+0}(i)$ is within the range $(\theta_t^-(i),\theta_t^+(i))$. If the air-conditioner is on proper operation mode, we can obtain the cooling period $\Delta\tau_{\text{on},t}(i)$, the standby cycle $\Delta\tau_{\text{off},t}(i)$, and the operational cycle $\Delta\tau_{1,t}(i)$ by solving (C7).

$$\Delta\tau_{1,t}(i)=\Delta\tau_{\text{on},t}(i)+\Delta\tau_{\text{off},t}(i) \tag{C9}$$

$$\Delta\tau_{\text{on},t}(i)=R(i)C(i)\ln\frac{\theta_t^+(i)+\eta(i)P_{\text{TCL,N}}(i)R(i)-\theta_{\text{out},t}(i)}{\theta_t^-(i)+\eta(i)P_{\text{TCL,N}}(i)R(i)-\theta_{\text{out},t}(t)} \tag{C10}$$

$$\Delta\tau_{\text{off},t}(i)=R(i)C(i)\ln\frac{\theta_{\text{out},t}(i)-\theta_t^-(i)}{\theta_{\text{out},t}(i)-\theta_t^+(i)} \tag{C11}$$

Given the initial indoor temperature $\theta_{\text{in},t+0}(i)$, the duration $\Delta\tau_{2,t}(i)$ from $\Delta\tau$=0 to the time when the state of air-conditioner first changes is calculated as (C12). Then, the average active power $P_{\text{TCL,in},t}(i)$ in the period $[t,t+1]$ is expressed as follows.

$$\Delta\tau_{2,t}(i)=\begin{cases}R(i)C(i)\ln\dfrac{\theta_{\text{in},t+0}(i)+\eta(i)P_{\text{TCL,N}}(i)R(i)-\theta_{\text{out},t}(i)}{\theta_t^-(i)+\eta(i)P_{\text{TCL,N}}(i)R(i)-\theta_{\text{out},t}(i)} & y_t(i)=1\\ R(i)C(i)\ln\dfrac{\theta_{\text{out},t}(i)-\theta_{\text{in},t+0}(i)}{\theta_{\text{out},t}(i)-\theta_t^+(i)} & y_t(i)=0\end{cases} \tag{C12}$$

$$P_{\text{TCL,in},t}(i)=y_t(i)P_{\text{TCL,in},t}(i)\big|_{y_t(i)=1}+(1-y_t(i))P_{\text{TCL,in},t}(i)\big|_{y_t(i)=0} \tag{C13}$$

$$P_{\text{TCL,in},t}(i)\big|_{y_t(i)=1}=\begin{cases}\eta(i)P_{\text{TCL,N}}(i)/\Delta t & \Delta t\in[0,\Delta\tau_{2,t}(i)]\\ \eta(i)P_{\text{TCL,N}}(i)(\Delta\tau_{2,t}(i)+k_1\Delta\tau_{\text{on},t}(i))/\Delta t & \Delta t\in(\Delta\tau_{2,t}(i)+k_1\Delta\tau_{1,t}(i),\Delta\tau_{2,t}(i)+k_1\Delta\tau_{1,t}(i)+\Delta\tau_{\text{off},t}(i)]\\ \eta(i)P_{\text{TCL,N}}(i)\left[\Delta t-(k_1+1)\Delta\tau_{\text{off},t}(i)\right]/\Delta t & \Delta t\in(\Delta\tau_{2,t}(i)+k_1\Delta\tau_{1,t}(i)+\Delta\tau_{\text{off},t}(i),\Delta\tau_{2,t}(i)+(k_1+1)\Delta\tau_{1,t}(i)]\end{cases} \tag{C14}$$

$$P_{\text{TCL,in},t}(i)\big|_{y_t(i)=0}=\begin{cases}0 & \Delta t\in[0,\Delta\tau_{2,t}(i)]\\ \eta(i)P_{\text{TCL,N}}(i)(\Delta t-\Delta\tau_{2,t}(i)-k_1\Delta\tau_{\text{off}}^{\text{no}})/\Delta t & \Delta t\in(\Delta\tau_{2,t}(i)+k_1\Delta\tau_{1,t}(i),\Delta\tau_{2,t}(i)+k_1\Delta\tau_{1,t}(i)+\Delta\tau_{\text{on},t}(i)]\\ \eta(i)P_{\text{TCL,N}}(i)(k_1+1)\Delta\tau_{\text{on},t}(i)/\Delta t & \Delta t\in(\Delta\tau_{2,t}(i)+k_1\Delta\tau_{1,t}(i)+\Delta\tau_{\text{on},t}(i),\Delta\tau_{2,t}(i)+(k_1+1)\Delta\tau_{1,t}(i)]\end{cases} \tag{C15}$$

If the air-conditioner is scheduled to supply the upward flexibility, $\theta_{\text{in},t+\tau}(i)$ will increase until $\theta_{\text{in},t+\tau}(i)\geq\theta^+_{\text{user},t}(i)$, which lasts for a period $\Delta\tau^+_{2,t}(i)$. Then, $\theta_{\text{in},t+\tau}(i)$ varies periodically in the range of $[\theta_t^+(i),\theta^+_{\text{user},t}(i)]$. The cooling cycle $\Delta\tau^+_{\text{on},t}(i)$, standby cycle $\Delta\tau^+_{\text{off},t}(i)$ and operation cycle $\Delta\tau^+_{1,t}(i)$ are given as:

$$\Delta\tau^+_{1,t}(i)=\Delta\tau^+_{\text{on},t}(i)+\Delta\tau^+_{\text{off},t}(i) \tag{C16}$$

$$\Delta\tau^+_{\text{on},t}(i)=R(i)C(i)\ln\frac{\theta^+_{\text{user},t}(i)+\eta(i)P_{\text{TCL,N}}(i)R(i)-\theta_{\text{out},t}(i)}{\theta_t^+(i)+\eta(i)P_{\text{TCL,N}}(i)R(i)-\theta_{\text{out},t}(i)} \tag{C17}$$

$$\Delta\tau^+_{\text{off},t}(i)=R(i)C(i)\ln\frac{\theta_{\text{out},t}(i)-\theta_t^+(i)}{\theta_{\text{out},t}(i)-\theta^+_{\text{user},t}(i)} \tag{C18}$$

$$P^+_{\text{TCL},t}(i)=\begin{cases}0 & \Delta t\in(0,\Delta\tau^+_{2,t}(i)]\\ \eta(i)P_{\text{TCL,N}}(i)(\Delta t-\Delta\tau^+_{2,t}(i)-k_1^+\Delta\tau^+_{\text{off},t}(i))/\Delta t & \Delta t\in(\Delta\tau^+_{2,t}(i)+k_1^+\Delta\tau^+_{1,t}(i),\leq\Delta\tau^+_{2,t}(i)+k_1^+\Delta\tau^+_{1,t}(i)+\Delta\tau^+_{\text{on},t}(i)]\\ \eta(i)P_{\text{TCL,N}}(i)(k_1^++1)\Delta\tau^+_{\text{on},t}(i)/\Delta t & \Delta t\in(\Delta\tau^+_{2,t}(i)+k_1^+\Delta\tau^+_{1,t}(i)+\Delta\tau^+_{\text{on},t}(i),\Delta\tau^+_{2,t}(i)+(k_1^++1)\Delta\tau^+_{1,t}(i)]\end{cases} \tag{C20}$$

$$\Delta\tau^+_{2,t}(i)=R(i)C(i)\ln\frac{\theta_{\text{out},t}(i)-\theta_{\text{in},t+0}(i)}{\theta_{\text{out},t}(i)-\theta^+_{\text{user}}(i)} \tag{C19}$$

We use $P^+_{\text{TCL},t}(i)$ to represent the average active power under the standby instruction. Thus, the maximum schedulable upward flexibility $F^+_{\text{TCL,max},t}(j)$ of TCL cluster is given as:

$$F^+_{\text{TCL,max},t}(j)=\sum_{i\in\{k|m_c(k)=j\cup r_t(k)=1\}}P_{\text{TCL,in},t}(i)-P^+_{\text{TCL},t}(i) \tag{C21}$$

If the air-conditioner is scheduled to supply the downward flexibility, $\theta_{\text{in},t+\tau}(i)$ will decrease until $\theta_{\text{in},t+\tau}(i)\leq\theta^-_{\text{user},t}(i)$, which lasts for a period $\Delta\tau^-_{2,t}(i)$. Then, $\theta_{\text{in},t+\tau}(i)$ varies periodically between $\theta^-_{\text{user},t}(i)$ and $\theta_t^-(i)$. The cooling cycle $\Delta\tau^-_{\text{on},t}(i)$, standby cycle $\Delta\tau^-_{\text{off},t}(i)$ and operation cycle $\Delta\tau^-_{1,t}(i)$ are given as (C22)~(C24).

$$\Delta\tau^-_{1,t}(i)=\Delta\tau^-_{\text{on},t}(i)+\Delta\tau^-_{\text{off},t}(i) \tag{C22}$$

$$\Delta\tau_{\text{on},t}^{-}(i)=R(i)C(i)\ln\frac{\theta_t^{-}(i)+\eta(i)P_{\text{TCL,N}}(i)R(i)-\theta_{\text{out},t}(i)}{\theta_{\text{user}t}^{-}(i)+\eta(i)P_{\text{TCL,N}}(i)R(i)-\theta_{\text{out},t}(i)} \quad \text{(C23)}$$

$$\Delta\tau_{\text{off},t}^{-}(i)=R(i)C(i)\ln\frac{\theta_{\text{out},t}(i)-\theta_{\text{user}}^{-}(i)}{\theta_{\text{out},t}(i)-\theta^{-}(i)} \quad \text{(C24)}$$

$$\Delta\tau_{2,t}^{-}(i)=R(i)C(i)\ln\frac{\theta_{\text{in},t+0}(i)+\eta(i)P_{\text{TCL,N}}(i)R(i)-\theta_{\text{out},t}(i)}{\theta_{\text{user},t}^{-}(i)+\eta(i)P_{\text{TCL,N}}(i)R(i)-\theta_{\text{out},t}(i)} \quad \text{(C25)}$$

$$P_{\text{TCL},t}^{-}(i)=\begin{cases}\eta(i)P_{\text{TCL,N}}(i)/\Delta t & \Delta t\in[0,\Delta\tau_{2,t}^{-}(i)]\\ \eta(i)P_{\text{TCL,N}}(i)(\Delta\tau_{2,t}^{-}(i)+k_1^{-}\Delta\tau_{\text{on},t}^{-}(i))/\Delta t & \Delta t\in(\Delta\tau_{2,t}^{-}(i)+k_1^{-}\Delta\tau_{1,t}^{-}(i),\Delta\tau_{2,t}^{-}(i)+k_1^{-}\Delta\tau_{1,t}^{-}(i)+\Delta\tau_{\text{off},t}^{-}(i)]\\ \eta(i)P_{\text{TCL,N}}(i)\left[\Delta t-(k_1^{-}+1)\Delta\tau_{\text{off},t}^{-}(i)\right]/\Delta t & \Delta t\in(\Delta\tau_{2,t}^{-}(i)+k_1^{-}\Delta\tau_{1,t}^{-}(i)+\Delta\tau_{\text{off},t}^{-}(i),\Delta\tau_{2,t}^{-}(i)+(k_1^{-}+1)\Delta\tau_{1,t}^{-}(i)]\end{cases} \quad \text{(C26)}$$

We use $P_{\text{TCL},t}^{-}(i)$ to represent the average active power under cooling instruction. As such, the maximum schedulable downward flexibility $F_{\text{TCL,max},t}^{-}(j)$ of TCL cluster is given as:

$$F_{\text{TCL,max},t}^{-}(j)=\sum_{i\in\{k|m_c(k)=j\cup r_t(k)=1\}}P_{\text{TCL},t}^{-}(i)-P_{\text{TCL,in},t}(i) \quad \text{(C27)}$$

If $\theta_{\text{in},t+0}(i)\geq\theta_t^{+}(i)$, the air-conditioner will not respond to the standby instruction, whose maximum schedulable downward flexibility can be calculated by (C27). In the same way, if $\theta_{\text{in},t+0}(i)\leq\theta_t^{-}(i)$, the air-conditioner has no downward flexibility to be scheduled, whose maximum upward flexibility can be calculated by (C21). Finally, we can obtain the maximum schedulable flexibility of TCL cluster:

$$F_{\text{TCL,max},t}^{+}(j)=\sum_{i\in\left\{k\,\middle|\,\substack{m_c(k)=j\cup r_t(k)=1\cup\\ \theta_{\text{in},t+0}(k)\in[\theta_{\text{user},t}^{-}(k),\theta_t^{+}(k))}\right\}}P_{\text{TCL,in},t}(i)-P_{\text{TCL},t}^{+}(i) \quad \text{(C28)}$$

$$F_{\text{TCL,max},t}^{-}(j)=\sum_{i\in\left\{k\,\middle|\,\substack{m_c(k)=j\cup r_t(k)=1\cup\\ \theta_{\text{in},t+0}(k)\in(\theta_t^{-}(k),\theta_{\text{user},t}^{+}(k)]}\right\}}P_{\text{TCL},t}^{-}(i)-P_{\text{TCL,in},t}(i) \quad \text{(C29)}$$

When TCL cluster is scheduled to supply upward flexibility or downward flexibility ($F_{\text{TCL},t}^{+}(j)/F_{\text{TCL},t}^{-}(j)$), its active power consumption will be changed into (C30):

$$P_{\text{TCL},t}(j)=\sum_{i\in\{k|m_c(k)=j\cup r_t(k)=1\}}P_{\text{TCL,in},t}(i)-F_{\text{TCL},t}^{+}(j)+F_{\text{TCL},t}^{-}(j) \quad \text{(C30)}$$

where $P_{\text{TCL,in},t}(i)$ is the average active power of air-conditioner during scheduling period $[t,t+1]$ on the proper operation.

C. Maximum Schedulable Flexibility of DG Cluster

We use $F_{\text{DPV,max},t}^{-}(j)$ and $F_{\text{DWP,max},t}^{-}(j)$ to denote the maximum schedulable downward flexibility of DPV and DWP cluster. When DPV or DWP cluster is scheduled to supply downward flexibility, its active power ($P_{\text{DPV},t}(j)/P_{\text{DWP},t}(j)$) is altered into:

$$\begin{cases}P_{\text{DPV},t}(j)=F_{\text{DR},t}^{-}(j)-P_{\text{DPV,out},t}(j)\\ P_{\text{DWP},t}(j)=F_{\text{DWP},t}^{-}(j)-P_{\text{DWP,out},t}(j)\end{cases} \quad \text{(C31)}$$

where $P_{\text{DPV,out},t}(j)$ and $P_{\text{DWP,out},t}(j)$ are the real-time active power of DPV and DWP cluster at the scheduling time t.

The operational data of DES is given as $Z_{\text{DES},t}(i)=\{U_{\text{DES}}(i), \xi_{\text{DES}}(i), E_{\text{DES},t}(i), m_e(i)\}$. In the set $Z_{\text{DES},t}(i)$, $U_{\text{DES}}(i)$ represents the storage capacity, $\xi_{\text{DES}}(i)$ is the charging and discharging efficiency, $E_{\text{DES},t}(i)$ is the SOC of DES, $m_e(i)$ is the number of DES cluster that it belongs to. Then, the maximum schedulable upward flexibility and downward flexibility of DES cluster ($F_{\text{DES,max},t}^{+}(j)$ & $F_{\text{DES,max},t}^{-}(j)$) are given as (C32). $P_{\max}(j)$ is the maximum charging/discharging power of DES cluster. With the scheduled upward and downward flexibility ($F_{\text{DES},t}^{+}(j)$, $F_{\text{DES},t}^{-}(j)$), we can obtain the active power $P_{\text{DES},t}(j)$ as:

$$\begin{cases}F_{\text{DES,max},t}^{+}(j)=\sum_{i\in\{k|m_e(k)=j\}}\min\left\{\frac{E_{\text{DES},t}(i)U_{\text{DES}}(i)}{\Delta t},P_{\max}(m_e(i))\right\}\\ F_{\text{DES,max},t}^{-}(j)=\sum_{i\in\{k|m_e(k)=j\}}\min\left\{\frac{(1-E_{\text{DES},t}(i))U_{\text{DES}}(i)}{\Delta t},P_{\max}(m_e(i))\right\}\end{cases} \quad \text{(C32)}$$

$$P_{\text{DES},t}(j)=F_{\text{DES},t}^{-}(j)-F_{\text{DES},t}^{+}(j) \quad \text{(C33)}$$

APPENDIX D

A. EV Operational State

With reference to [40]-[41], the parking generation rate is introduced to describe the characteristic of EVs. As presented in Fig. D1 and Fig. D2, we artificially divide these districts into the residential districts, the commercial districts, and the industrial districts. The parking generation rate of different types of districts is shown as Fig. D5, and the traveling distance between districts are also given in Table DIII and DIV. There are a total of 1400/1300 vehicles in the simulation of IEEE 33/69 buses systems, which can be classified into two types, namely the compact EV and the ordinary EV, whose essential data are given in Table DV. We set the number of parking spot for each EV cluster as the value 20. Based on the different types of districts, the quantity of DSR clusters within each district is given in Table DVI and DVII. Besides, the maximum charging and discharging power of all EV clusters is set to 10 kW.

B. TCL Operational State

In reality, the air-conditioner can be scheduled only when it is turned on by user. We assume that each house is shared by at least two users and has one air-conditioners. In order to simplify the simulation process, all houses within each district accommodate the same number of users. Each house is shared by 5 users in IEEE 33-buses system, whereas the above number is the value 2 to 10 in IEEE 69-buses system. The number of air-conditioners within each TCL cluster is set to the value 4. According to these assumptions, the load transfer model of TCLs is built based on the mobile energy storage model of EVs. The certain quantity of TCLs within the power supply district should be randomly selected to change the value of $r_t(i)$ to 1, such that the quantity of TCLs is equivalent to round up the fraction the quantity of EVs over the quantity of houses within the same district. Similarly, the air-conditioners can also be classified into three types, whose parameters are uniformly distributed in the certain range shown in Table DVIII. The outdoor temperature is also given in Fig. D6, which is constant for all air-conditioners.

C. Principle for Selecting Essential Paraments of Edge Nodes

This principle is proposed to determine both the quantity and the installation location of edge nodes for a distribution network based on another distribution network with different size. First of all, the quantity of edge nodes should be decided. Suppose that the quantity of edge nodes for the referenced distribution network is p_1. Then, the quantity of edge nodes for the distribution network, which is waiting for being solved, is denoted by variable p_2. The above two variables are linked by the quantity ($|S_1|_{\text{non-zero}}$ and $|S_2|_{\text{non-zero}}$) of power districts with non-zero DSR clusters contained in their respective networks ($\boldsymbol{S}_1$ and $\boldsymbol{S}_2$), which is given as $p_1 : |S_1|_{\text{non-zero}} \approx p_2 : |S_2|_{\text{non-zero}}$. In this way, the edge calculation power, which is used for the flexibility scheduling of all districts, may tends to be equal in the distribution networks with different sizes. For the distribution networks utilized in the simulation, we can obtain $p_2 = 10$ with the known data $|S_1|_{\text{non-zero}} = 32$, $|S_2|_{\text{non-zero}} = 38$, $p_1 = 8$. Given the quantity of edge nodes, the second thing is to decide the installation location of these edge nodes, which is divided into two steps. The first step is to obtain the relevant paraments of the referenced distribution network. We first adopt the result of offloading strategy in the upload stage as reference, so as to calculate the transmission distance and the average quantity of wired links H_1 from the power districts to their corresponding edge nodes in the referenced network. Besides the transmission distance, the selection of edge nodes also has great correlation with the computation delay of districts. Thus, the quantity of DSR clusters ($|N_{\text{all}}(s)|$) is taken as the weight of transmission delay for reflecting the impact of computation delay. Then, the weighted value of transmission delay equals to the product of DSR clusters quantity and transmission delay, and the sum of weighted value ($L_{\text{TD},1}$) can also be obtained. Since the distribution networks with different sizes have difference in the quantity of DSR cluster and the distance of wired links, the weighted value $L_{\text{TD},2}$ of another network is shown as:

$$\frac{L_{\text{TD},2}}{g_1} = \frac{L_{\text{TD},1} \sum\limits_{s\in S_2} |N_{\text{all}}(s)| \sum\limits_{(a,b)\in\pi_2(i,j)} d(a,b) / |S_2|}{g_2 \sum\limits_{s\in S_1} |N_{\text{all}}(s)| \sum\limits_{(a,b)\in\pi_1(i,j)} d(a,b) / |S_1|}. \tag{D1}$$

where g_1 and g_2 represent the total quantity of districts contained within the radiation scope of all edge nodes. Note that each power district can be counted repeatedly. In this paper, $L_{\text{TD},1}/g_1$=17.14, g_1=32, $L_{\text{TD,ideal},2}/g_2$=17.23, g_2=40.

The second step is to select the installation location of edge nodes in another distribution network. Although the method for calculating the weighted value $L_{\text{TD},2}$ has been introduced, it is still not clear which computation tasks of power districts the edge node should deal with. Thus, we take the average quantity of wired links H_1 as reference to determine the radiation scope of edge nodes. The variable H_2 is denoted by the maximum quantity of wired links between the edge node and the corresponding districts in the current network, which satisfies $H_1 : |S_1| \approx H_2 : |S_2|$. In the simulation, H_1≈1, H_2≈2. If the minimum quantity of wired links between the edge node and the district is higher than H_2, then the district will not in the radiation scope of this edge node. In this way, we can obtain the radiation scope of an edge node when its installation location has been determined. Besides the above requirements, each power district should be involved in the radiation scope of one edge node at least. According to the above settings, we manually determine the installation location of edge nodes in IEEE 69 buses system, which is shown in Fig. D2. The relevant key parameters are given in Table DI and Table DXI. The sum of all weighted value $L_{\text{TD,actual},2}/g_2$ equals to 17.44, which is close to the ideal value, i.e., $L_{\text{TD,ideal},2}/g_2$=17.23. Hence, the following installation locations set for edge nodes are rational.

TABLE DI
RELEVANT PARAMETERS FOR THE INSTALLATION LOCATION OF EDGE NODES

Location	Radiation scope	Weighted value	Location	Radiation scope	Weighted value
	38	5.20		10	4.80
(e_1, 36)	39	8.00		11	27.60
(e_1, 37)	35	2.80	(e_6, 10)	65	1.80
	36	0.80		66	3.60
(e_2, 42)	44	14.70		67	8.10
(e_2, 43)	45	23.10		53	5.20
	32	7.20	(e_7, 55)	54	3.60
(e_3, 29)	28	5.20	(e_7, 56)	58	22.00
(e_3, 30)	27	7.60		60	147.00
	49	31.00	(e_8, 61)	61	3.20
(e_4, 48)	48	31.00	(e_8, 62)	63	44.00
(e_4, 49)	47	18.00		64	44.00
	6	5.60		13	1.40
	7	2.70	(e_9, 14)	15	12.80
(e_5, 6)	8	21.70	(e_9, 15)	16	26.00
(e_5, 7)	9	21.00		17	43.00
	50	9.10		20	44.00
		31.50	(e_{10}, 23)	23	1.80
(e_6, 9)	8	4.90	(e_{10}, 22)	25	7.20
	9	1.80		26	4.60

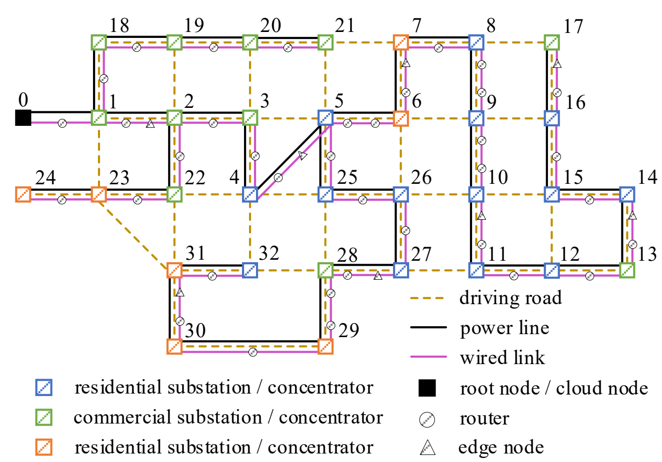

Fig.D1 IEEE 33-buses test system and corresponding communication network.

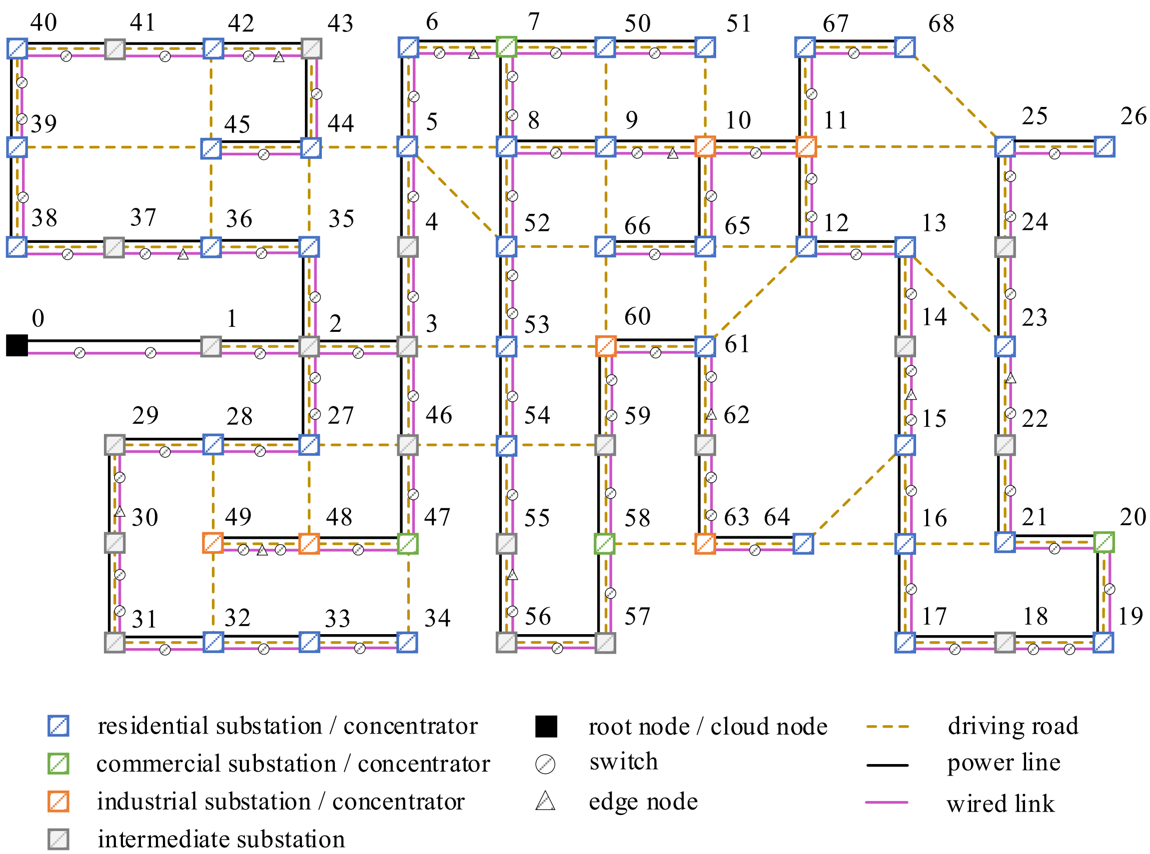

Fig.D2 IEEE 69-buses test system and corresponding communication network.

D. *Initial Operational Data and Simulation Results*

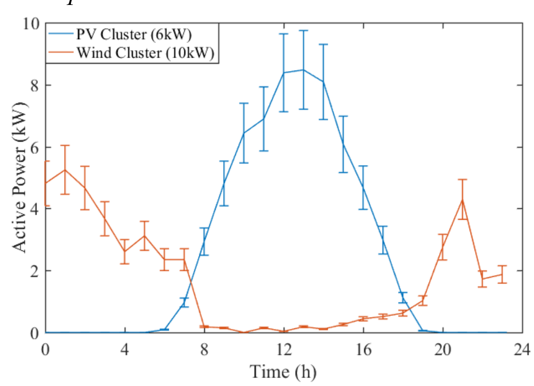

Fig.D3 Day-ahead output of 6kW PV and 10kW wind power ($\cos\varphi_{DPV}(j)=\cos\varphi_{DWP}(j)=0.95$).

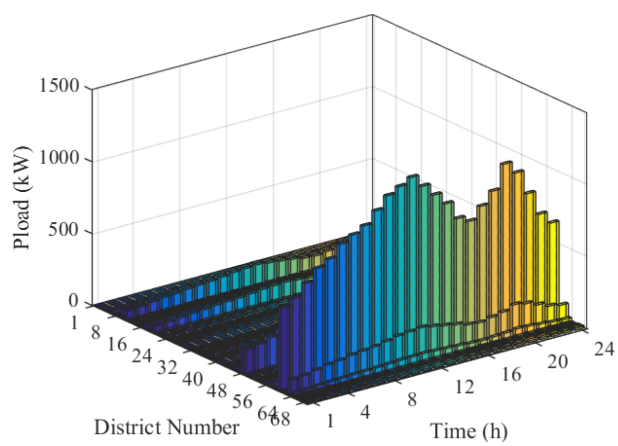

(a2) active power of load (IEEE 69 buses system)

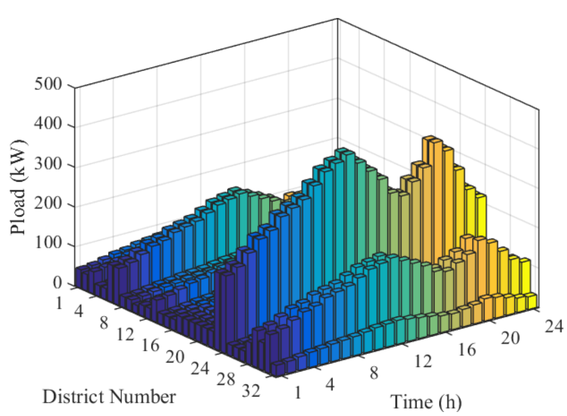

(a1) active power of load (IEEE 33 buses system)

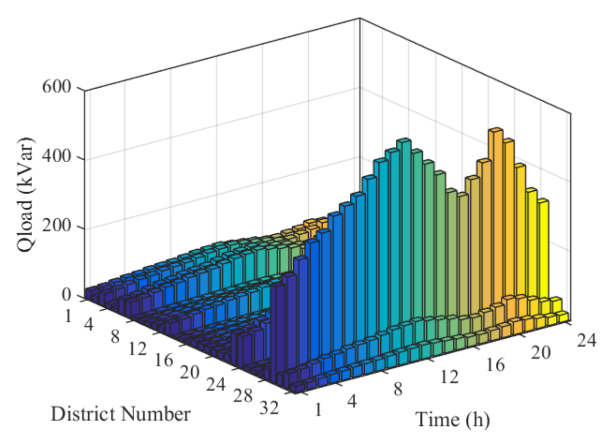

(b1) reactive power of load (IEEE 33 buses system)

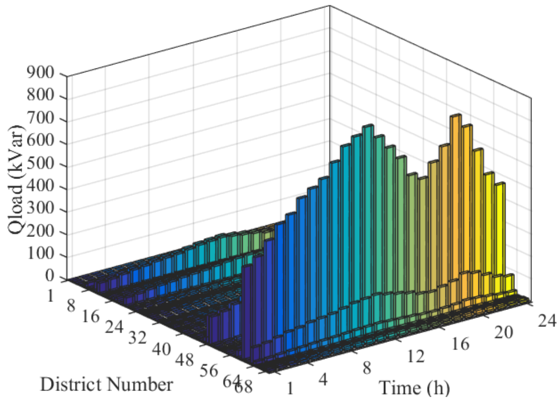

(b2) reactive power of load (IEEE 69 buses system)

Fig.D4 Day-ahead forecasted output of all power supply districts

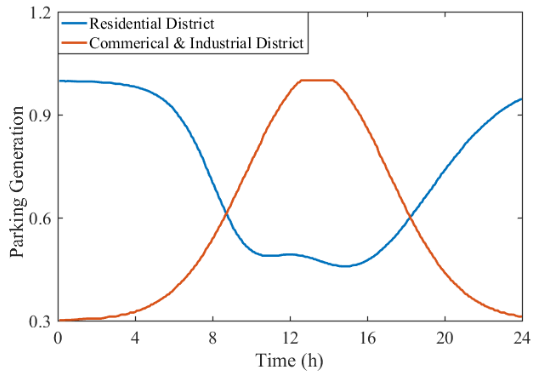

Fig.D5 Typical curve of parking generation rate for all types of power supply districts on working days.

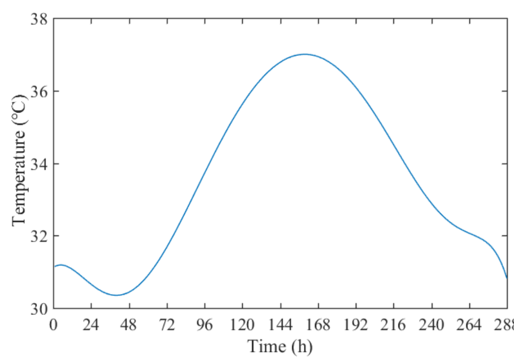

Fig.D6 Real-time outdoor temperature in the location of distribution network.

TABLE DIII
TRAVELING DISTANCE BETWEEN DISTRICTS (IEEE 33 BUSES SYSTEM)

Road	Distance/km	Road	Distance/km	Road	Distance/km
(1, 2)	1.00	(6, 26)	2.20	(16, 17)	1.20
(1, 18)	0.80	(7, 8)	0.80	(18, 19)	0.80
(1, 23)	1.50	(7, 21)	2.60	(19, 20)	1.10
(2, 19)	0.70	(8, 9)	2.00	(20, 21)	1.20
(2, 22)	1.50	(8, 17)	2.00	(22, 23)	1.20
(2, 3)	1.50	(9, 10)	2.00	(22, 31)	1.10
(3, 4)	0.50	(9, 16)	2.00	(23, 24)	0.60
(3, 5)	1.50	(10, 11)	0.60	(25, 26)	1.50
(3, 20)	2.30	(10, 15)	1.00	(25, 28)	0.80
(4, 22)	1.50	(10, 26)	1.20	(26, 27)	0.40
(4, 25)	1.00	(11, 12)	1.40	(27, 28)	1.80
(4, 32)	1.00	(11, 27)	1.00	(28, 29)	2.70
(5, 6)	2.00	(12, 13)	1.10	(28, 32)	1.20
(5, 21)	2.50	(12, 15)	1.10	(29, 30)	0.80
(5, 25)	0.60	(13, 14)	0.90	(30, 31)	0.70
(6, 7)	1.80	(14, 15)	0.60	(31, 23)	1.00
(6, 9)	1.40	(15, 16)	1.70	(32, 32)	1.60

TABLE DII
UNIT PRICE OF DSRS FOR FLEXIBILITY SCHEDULING

Time/h	EV/ ($/kWh)	TCL/ ($/kWh)	DPV/ ($/kWh)	DWP/ ($/kWh)	DES/ ($/kWh)
0:00~8:00	0.30	0.20	0.30	1.05	0.40
8:00~12:00 17:00~21:00	1.08	0.82	0.70	1.55	1.00
12:00~17:00 21:00~24:00	0.70	0.55	0.40	1.15	0.65

TABLE DIV
TRAVELING DISTANCE BETWEEN POWER SUPPLY DISTRICT
(IEEE 69 BUSES SYSTEM)

Road	Distance/km	Road	Distance/km	Road	Distance/km
(1, 2)	1.50	(16, 17)	1.70	(40, 41)	1.20
(2, 3)	1.50	(16, 21)	1.50	(41, 42)	1.80
(2, 35)	0.80	(16, 64)	0.90	(42, 43)	1.50
(2, 27)	2.20	(17, 18)	1.00	(42, 45)	1.50
(3, 4)	1.40	(18, 19)	2.00	(43, 44)	1.50
(3, 46)	1.20	(19, 20)	1.60	(44, 45)	1.20
(3, 53)	1.90	(20, 21)	1.60	(46, 47)	1.30
(4, 5)	0.90	(21, 22)	1.80	(46, 54)	1.70
(5, 6)	0.70	(22, 23)	1.20	(47, 48)	1.00
(5, 8)	1.30	(23, 24)	0.90	(48, 49)	2.00
(5, 52)	2.20	(24, 25)	2.10	(50, 51)	1.10
(5, 44)	2.00	(25, 26)	1.00	(51, 10)	1.70
(6, 7)	1.10	(25, 68)	2.40	(52, 53)	2.00
(7, 8)	2.80	(27, 28)	1.20	(52, 66)	1.80
(7, 50)	1.00	(27, 46)	1.30	(53, 54)	0.80
(8, 9)	0.40	(27, 48)	1.00	(53, 60)	1.20
(8, 52)	1.80	(28, 29)	1.60	(54, 55)	1.20
(9, 10)	0.70	(28, 49)	1.30	(54, 59)	0.70
(9, 50)	1.00	(29, 30)	1.40	(55, 56)	1.20
(9, 66)	1.40	(30, 31)	2.20	(56, 57)	0.80
(10, 11)	1.90	(31, 32)	1.00	(57, 58)	0.60
(10, 65)	0.50	(32, 33)	1.50	(58, 59)	0.90
(11, 25)	3.00	(32, 49)	2.60	(58, 63)	1.40
(11, 12)	2.50	(33, 34)	1.50	(59, 60)	2.10
(11, 67)	0.40	(34, 47)	1.20	(60, 61)	0.70
(12, 13)	1.90	(35, 36)	1.00	(61, 62)	0.90
(12, 61)	1.70	(35, 44)	1.10	(61, 65)	1.40
(12, 65)	1.80	(36, 37)	1.40	(62, 63)	2.10
(13, 14)	1.00	(36, 45)	2.40	(63, 64)	1.10
(13, 23)	2.40	(37, 38)	1.60	(65, 66)	0.90
(14, 15)	2.00	(38, 39)	1.40	(67, 68)	1.50
(15, 16)	1.00	(39, 40)	2.20	(60, 66)	1.50
(15, 64)	1.40	(39, 45)	3.00		

TABLE DV
ESSENTIAL DATA FOR BOTH TYPES OF EVS

	U_{EV}/(kW·h)	ξ_{EV}/%	E_{min}/%	v_1/(km·h^{-1})
Compact type	18.00	95.00	30.00	36.00
Ordinary type	30.00	95.00	20.00	48.00

Note: v_1 represents the average driving speed of EV.

TABLE DVI
QUANTITY OF (EV & TCL)/(DPV, DWP & DES) CLUSTERS WITHIN POWER SUPPLY DISTRICTS (IEEE 33 BUSES SYSTEM)

District No.	Cluster Quantity	District No.	Cluster Quantity
1	2 / 2	17	2 / 2
2	2 / 2	18	2 / 2
3	3 / 2	19	2 / 2
4	3 / 1	20	2 / 2
5	3 / 1	21	2 / 2
6	2 / 4	22	2 / 2
7	2 / 4	23	4 / 8
8	3 / 1	24	4 / 8
9	3 / 1	25	3 / 1
10	2 / 1	26	3 / 1
11	3 / 1	27	3 / 1
12	3 / 1	28	3 / 2
13	3 / 2	29	2 / 4
14	3 / 1	30	2 / 3
15	3 / 1	31	2 / 4
16	3 / 1	32	3 / 1

TABLE DVII
QUANTITY OF EV/TCL/(DPV, DWP & DES) CLUSTERS WITHIN POWER SUPPLY DISTRICTS (IEEE 69 BUSES SYSTEM)

District No.	Cluster Quantity	District No.	Cluster Quantity
1	0 / 0 / 0	35	1 / 1 / 0
2	0 / 0 / 0	36	1 / 1 / 0
3	0 / 0 / 0	37	0 / 0 / 0
4	0 / 0 / 0	38	1 / 1 / 0
5	0 / 0 / 0	39	1 / 1 / 0
6	2 / 2 / 1	40	0 / 0 / 0
7	2 / 1 / 2	41	0 / 0 / 0
8	2 / 2 / 1	42	0 / 0 / 0
9	1 / 2 / 1	43	0 / 0 / 0
10	2 / 1 / 3	44	2 / 2 / 1
11	2 / 1 / 3	45	2 / 2 / 1
12	0 / 0 / 0	46	0 / 0 / 0
13	1 / 0 / 0	47	2 / 1 / 2
14	0 / 0 / 0	48	4 / 3 / 8
15	2 / 3 / 1	49	4 / 3 / 8
16	3 / 4 / 1	50	2 / 2 / 1
17	3 / 4 / 1	51	0 / 0 / 0
18	0 / 0 / 0	52	0 / 0 / 0
19	0 / 0 / 0	53	1 / 1 / 0
20	3 / 2 / 2	54	1 / 1 / 0
21	0 / 0 / 0	55	0 / 0 / 0
22	0 / 0 / 0	56	0 / 0 / 0
23	1 / 2 / 0	57	0 / 0 / 0
24	0 / 0 / 0	58	3 / 2 / 2
25	1 / 1 / 0	59	0 / 0 / 0
26	0 / 1 / 0	60	13 / 10 / 25
27	1 / 1 / 0	61	2 / 2 / 0
28	1 / 1 / 0	62	0 / 0 / 0
29	0 / 0 / 0	63	3 / 2 / 5
30	0 / 0 / 0	64	3 / 4 / 1
31	0 / 0 / 0	65	1 / 1 / 0
32	1 / 1 / 0	66	1 / 2 / 0
33	0 / 0 / 0	67	1 / 2 / 0
34	0 / 0 / 0	68	1 / 2 / 0

Note: these power districts have no DSR clusters because their load is either too small or zero.

TABLE DVIII
ESSENTIAL DATA FOR THREE TYPES OF AIR-CONDITIONERS

Type	R/(°C/kW)	C/(kWh/°C)	$\eta P_{\mathrm{TCL,N}}$/kW
I	[6.10, 8.14]	[0.14, 0.24]	[2.83, 3.33]
II	[4.76, 6.36]	[0.13, 0.23]	[6.50, 7.50]
III	[1.50, 2.50]	[1.50, 2.50]	[16.00, 20.00]
Type	η	θ_{set}/°C	$\Delta\theta_{\mathrm{n}}$ & $\Delta\theta_{\mathrm{s}}$/°C
I	[2.80, 3.20]	[24.00, 26.00]	2.00 & 4.00
II	[2.60, 3.00]	[22.00, 24.00]	4.00 & 6.00
III	[2.60, 3.00]	[23.00, 25.00]	1.00 & 2.00

Note: θ_{set} represents the temperature set value of air-conditioner. $\Delta\theta_{\mathrm{n}}$ and $\Delta\theta_{\mathrm{s}}$ are used to denote the width of temperature dead zone when the air-conditioner is on the proper operation mode and the scheduled mode.

TABLE DIX
ESSENTIAL PARAMETERS OF DES CLUSTERS

U_{DES}/kW	$P_{\max}$/kW	ξ_{DES}/ %
[4.00, 6.00]	[2.00, 3.00]	86.00

Note: The installed capacity and charging / discharging power of each DES cluster obeys uniform distribution in a certain range.

TABLE DX
TRANSMISSION DISTANCE BETWEEN COMMUNICATION NODES EXCEPT END NODES (IEEE 33 BUSES SYSTEM)

Link	Distance/km	Link	Distance/km
(1, 2)	1.00	(25, 26)	1.50
(1, 18)	0.80	(26, 27)	0.40
(2, 3)	1.50	(27, 28)	1.80
(2, 22)	1.50	(28, 29)	2.70
(3, 4)	0.50	(29, 30)	0.80
(4, 5)	1.20	(30, 31)	0.70
(5, 6)	2.00	(31, 32)	1.60
(5, 25)	0.60	(0, 1)	1.40
(6, 7)	1.80	(e_1, 1)	0.40
(7, 8)	0.80	(e_1, 2)	0.60
(8, 9)	2.00	(e_2, 4)	0.60
(9, 10)	2.00	(e_2, 5)	0.60
(10, 11)	0.60	(e_3, 7)	1.00
(11, 12)	1.40	(e_3, 6)	0.80
(12, 13)	1.10	(e_4, 16)	0.80
(13, 14)	0.90	(e_4, 17)	0.40
(14, 15)	0.60	(e_5, 30)	0.40
(15, 16)	1.70	(e_5, 31)	0.30
(16, 17)	1.20	(e_6, 27)	0.80
(18, 19)	0.80	(e_6, 28)	1.00
(19, 20)	1.10	(e_7, 10)	0.20
(20, 21)	1.20	(e_7, 11)	0.40
(22, 23)	1.20	(e_8, 13)	0.50
(23, 24)	0.60	(e_8, 14)	0.40

Note: e_1~e_8 represents the edge nodes belonging to the set E.

TABLE DXI
TRANSMISSION DISTANCE BETWEEN COMMUNICATION NODES EXCEPT END NODES (IEEE 69 BUSES SYSTEM)

Link	Distance/km	Link	Distance/km
(1, 2)	1.50	(39, 40)	2.20
(2, 3)	1.50	(40, 41)	1.20
(2, 35)	0.80	(41, 42)	1.80
(2, 27)	2.20	(42, 43)	1.50
(3, 4)	1.40	(43, 44)	1.50
(3, 46)	1.20	(44, 45)	1.20
(4, 5)	0.90	(46, 47)	1.30
(5, 6)	0.70	(47, 48)	1.00
(6, 7)	1.10	(48, 49)	2.00
(7, 8)	2.80	(50, 51)	1.10
(7, 50)	1.00	(52, 53)	2.00
(8, 9)	0.40	(53, 54)	0.80
(8, 52)	1.80	(54, 55)	1.20
(9, 10)	0.70	(55, 56)	1.20
(10, 11)	1.90	(56, 57)	0.80
(10, 65)	0.50	(57, 58)	0.60
(11, 25)	3.00	(58, 59)	0.90
(11, 12)	2.50	(59, 60)	2.10
(11, 67)	0.40	(60, 61)	0.70
(12, 13)	1.90	(61, 62)	0.90
(13, 14)	1.00	(62, 63)	2.10
(14, 15)	2.00	(63, 64)	1.10
(15, 16)	1.00	(65, 66)	0.90
(16, 17)	1.70	(67, 68)	1.50
(17, 18)	1.00	(e_1, 36)	0.40
(18, 19)	2.00	(e_1, 37)	1.00
(19, 20)	1.60	(e_2, 42)	0.90
(20, 21)	1.60	(e_2, 43)	0.60
(21, 22)	1.80	(e_3, 29)	1.00
(22, 23)	1.20	(e_3, 30)	0.40
(23, 24)	0.90	(e_4, 48)	1.00
(24, 25)	2.10	(e_4, 49)	1.00
(25, 26)	1.00	(e_5, 6)	0.80
(27, 28)	1.20	(e_5, 7)	0.30
(28, 29)	1.60	(e_6, 9)	0.30
(29, 30)	1.40	(e_6, 10)	0.40
(30, 31)	2.20	(e_7, 55)	0.60
(31, 32)	1.00	(e_7, 56)	0.60
(32, 33)	1.50	(e_8, 61)	0.80
(33, 34)	1.50	(e_8, 62)	0.10
(35, 36)	1.00	(e_9, 14)	0.40
(36, 37)	1.40	(e_9, 15)	1.60
(37, 38)	1.60	(e_{10}, 23)	0.60
(38, 39)	1.40	(e_{10}, 22)	0.60

TABLE DXII
COMPUTATION DURATION IN BOTH UPLOAD STAGE AND DOWNLOAD STAGE (IEEE 33 BUSES SYSTEM)

Number of computing task	Computation duration/ms	Number of edge computation	Computation duration/ms
0	1448 / 25610	17	5.75 / 854.30
1	16.00 / 882.90	18	14.00 / 852.40
2	8.75 / 861.70	19	5.75 / 847.70
3	16.50 / 1013.1	20	7.00 / 855.10
4	13.50 / 1025.6	21	6.00 / 866.60
5	11.75 / 1059.5	22	7.25 / 849.40
6	6.50 / 918.80	23	20.50 / 1209.90
7	6.50 / 929.60	24	19.00 / 1234.90
8	9.75 / 970.00	25	9.25 / 981.80
9	7.50 / 972.20	26	6.75 / 963.30
10	6.75 / 855.60	27	6.25 / 994.00
11	16.25 / 950.80	28	16.00 / 1000.60
12	11.25 / 988.10	29	5.75 / 881.50
13	11.50 / 992.80	30	5.25 / 860.20
14	7.75 / 971.40	31	10.50 / 905.60
15	8.50 / 959.30	32	8.50 / 965.40
16	9.00 / 970.20		

Note: s=1 to 32 represent the number of edge computations, whereas the s=0 represents the cloud computation. For the edge computations, their computation duration is shown as t_{up} / t_{dw}, where t_{up} and t_{dw} are the duration in the upload and download process. For the cloud computation, the computation duration is shown as $t_{e\text{-}c}$ / t_{tra}, where the first term is the duration for the cloud calculation in the edge-cloud collaboration and the second term is the duration for cloud calculation in the traditional strategy.

TABLE DXIII
ESSENTIAL DATA FOR WIRED AND WIRELESS TRANSMISSION

Data size/ bytes	Time slot T/ ms	Link rate r/ kbit/s	Speed/ m/s	Service delay/ ms
200	1	500	1.8×10^5	3.8

Note: The data size corresponds to each DSR cluster.

TABLE DXIV
COMPUTATION DURATION IN BOTH UPLOAD STAGE AND DOWNLOAD STAGE (IEEE 69 BUSES SYSTEM)

Number of computing task	Computation duration/ms	Number of edge computation	Computation duration/ms
0	1892/41279	35	5.00 / 333.40
1	/	36	4.00 / 335.90
2	/	37	/
3	/	38	4.75 / 341.70
4	/	39	4.25 / 335.90
5	15.25 / 339.20	40	0.25 / 260.70
6	213.5 / 524.80	41	/
7	59.25 / 387.20	42	0.50 / 259.00
8	18.75 / 416.00	43	/
9	40.75 / 410.10	44	22.75 / 412.40
10	7.75 / 418.20	45	13.75 / 412.00
11	22.75 / 400.90	46	/
12	1.00 / 272.80	47	9.00 / 375.90
13	3.00 / 287.60	48	105.25 / 538.70
14	/	49	31.75 / 547.50
15	35.50 / 457.10	50	9.50 / 439.10
16	27.75 / 539.40	51	0.50 / 274.10
17	32.25 / 503.70	52	0.50 / 272.40
18	/	53	5.00 / 340.80
19	0.75 / 255.10	54	5.00 / 335.40
20	31.75 / 430.9	55	/
21	0.25 / 264.50	56	/
22	/	57	/
23	8.00 / 394.70	58	51.25 / 442.20
24	/	59	/
25	27.00 / 332.50	60	77.25 / 1122.30
26	13.50 / 320.80	61	18.00 / 405.20
27	6.75 / 335.00	62	/
28	26.50 / 323.80	63	18.00 / 456.00
29	/	64	17.75 / 532.40
30	/	65	7.00 / 338.30
31	/	66	5.75 / 344.40
32	7.75 / 343.40	67	60.50 / 394.70
33	0.50 / 258.30	68	9.50 / 405.50
34	0.75 / 263.30		

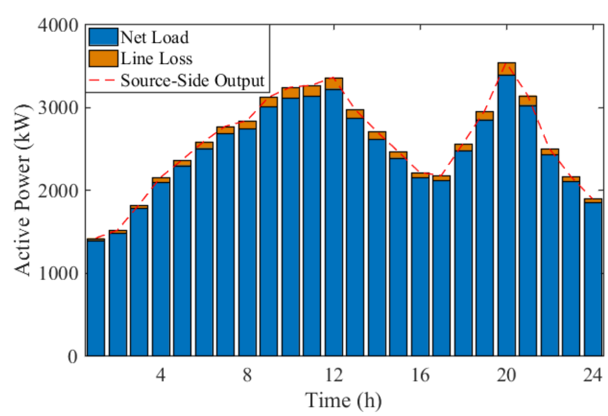

(a1) active source-side output (IEEE 33 buses system)

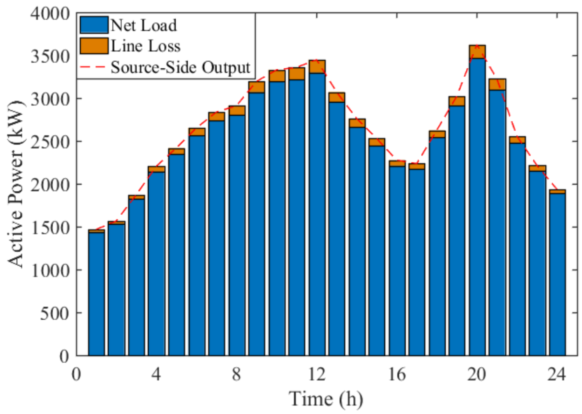

(a2) active source-side output (IEEE 69 buses system)

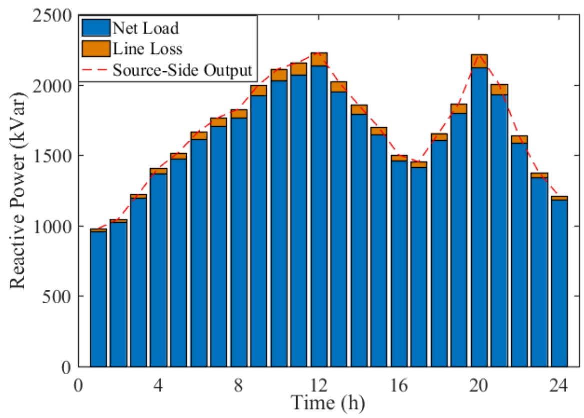

(b1) reactive source-side output (IEEE 33 buses system)

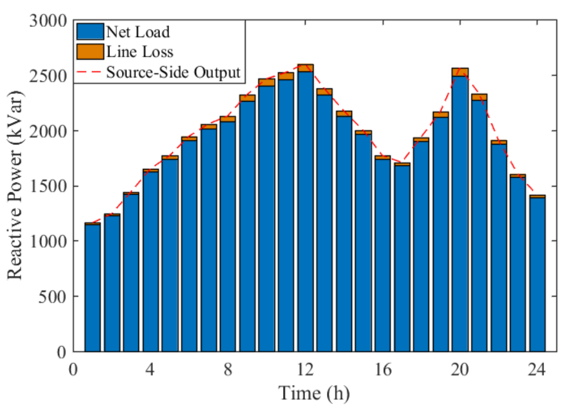

(b2) reactive source-side output (IEEE 69 buses system)

Fig. D7 The curve of day-ahead source-side output.

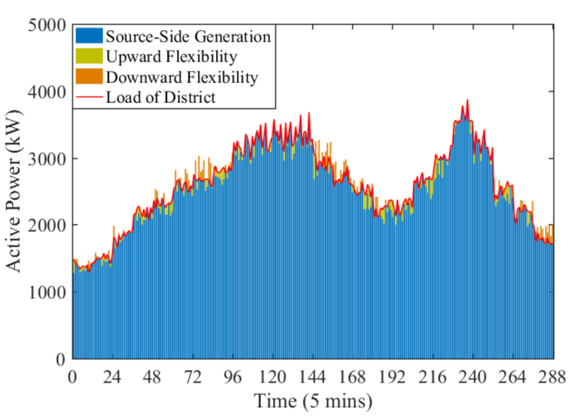

(a) Scheduled flexibility of IEEE 33 buses system

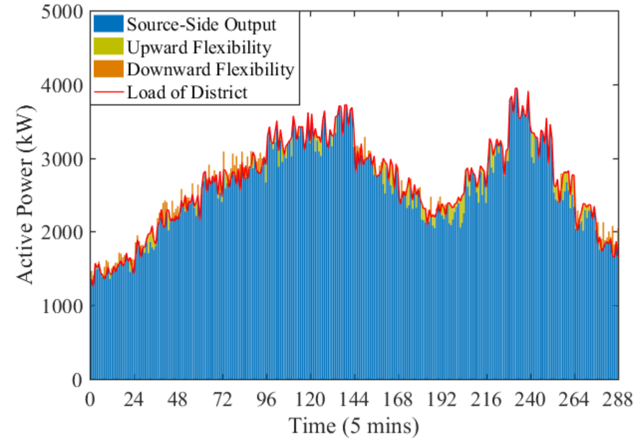

(b) Scheduled flexibility of IEEE 69 buses system

Fig. D8 The scheduled flexibility of distribution network.

TABLE DXV
RESULT OF OFFLOADING STRATEGY IN THE UPLOAD STAGE

	District No.	Arrival time t_a/ms	Waiting time t_s/ms	Upload delay D_{up}/ms
e_1	[18, 19, 1, 20, 21, 23]	[81.81, 81.81, 89.62, 89.63, 97.44, 313.03]	[0.00, 14.00, 11.94, 27.93, 27.11, 0.00]	[183.25,196.82, 205.00,235.45, 257.08,608.67]
e_2	[4, 5, 25, 2, 22, 3, 24]	[73.46, 81.28, 89.09, 89.63, 97.44, 98.79, 313.03]	[0.00, 5.68, 9.62, 18.33, 19.27, 25.18, 0.00]	[183.64,211.02, 235.90,211.98, 234.86,248.53 614.98]
e_3	[8, 9, 6, 7]	[81.28, 89.10, 133.71, 133.71]	[0.00, 1.93, 0.00, 6.50]	[226.79,249.94, 297.32,311.64]
e_4	[16, 17]	[73.47, 81.81]	[0.00, 0.66]	[272.95,292.91]
e_5	[32, 30, 31, 29]	[81.28, 107.41, 133.71, 141.52]	[0.00, 0.00, 0.00, 2.69]	[268.43,293.46, 352.02,268.43]
e_6	[27, 26, 28]	[73.47, 81.28, 98.79]	[0.00, 0.00, 0.00]	[207.65,215.96, 269.75]
e_7	[10, 11, 12]	[57.13, 73.46, 81.28]	[0.00, 0.00, 8.43]	[194.66,241.11, 268.00]
e_8	[14, 15, 13]	[73.47, 81.28, 98.79]	[0.00, 0.00, 0.00]	[256.06,280.25, 296.52]

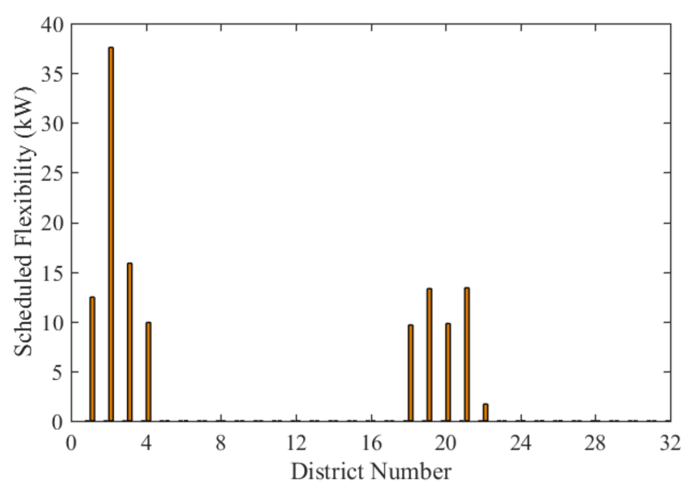

Fig. D9 Scheduled flexibility of each district at the scheduling time t=77.

TABLE DXVI
RESULT OF OFFLOADING STRATEGY IN THE UPLOAD STAGE AT SCHEDULING TIME T=77

Edge node	District No.	Arrival time t_a/ms	Waiting time t_s/ms	Download delay D_{dw}/ms
e_1	[3, 5, 8, 14]	[131.51, 143.57, 190.47, 284.28]	[0.00, 1001.04, 2013.63, 2889.83]	[1214.27, 2279.80, 3273.25, 4291.55]
e_2	[2, 22, 27, 9, 15]	[95.26, 110.90, 159.19, 174.86, 268.64]	[0.00, 846.06, 1647.17, 2625.51, 3503.92]	[1004.59, 1861.81, 2868.23, 3848.26, 4854.46]
e_3	[21, 11, 23]	[181.23, 182.67, 290.78]	[0.00, 865.16, 1707.85]	[1157.99, 2066.52, 3365.65]
e_4	[4, 25, 13, 30]	[190.48, 206.11, 209.68, 317.50]	[0.00, 1009.97, 1988.20, 2873.18]	[1346.50, 2328.29, 3260.34, 4236.99]
e_5	[20, 10, 7, 12, 17]	[208.49, 220.59, 231.28, 264.65, 349.21]	[0.00, 843.00, 1687.91, 2584.14, 3487.68]	[1208.81, 2039.20, 2974.15, 3978.93, 4875.51]
e_6	[1, 24]	[134.34, 322.03]	[0.00, 695.21]	[1111.75, 2432.68]
e_7	[19, 6, 28, 29, 31]	[181.24, 188.38, 225.31, 274.18, 305.43]	[0.00, 840.56, 1722.43, 2674.16, 3524.41]	[1154.74, 2038.03, 3064.91, 3970.84, 4892.07]
e_8	[18, 26, 16, 32]	[189.06, 198.29, 206.11, 299.72]	[0.00, 843.17, 1798.65, 2675.24]	[1182.89, 2119.54, 3027.20, 4105.86]

TABLE DXVII
RESULT OF OFFLOADING STRATEGY IN THE UPLOAD STAGE (IEEE 69 BUSES SYSTEM)

Edge node	District No.	Arrival time t_a/ms	Waiting time t_s/ms	Upload delay D_{up}/ms
e_1	[37, 36, 35, 38, 39, 27, 50, 49]	[3.82, 15.45, 15.46, 19.28, 19.29, 23.10, 68.41, 283.51]	[0.00, 0.00, 4.00, 5.18, 9.92, 10.36, 0.00, 0.00]	[23.16, 47.53, 52.54, 68.74, 76.82, 79.74, 164.72, 555.67]
e_2	[42, 40, 44, 45]	[3.81, 7.64, 56.94, 56.95]	[0.00, 0.00, 0.00, 22.74]	[39.19, 43.26, 170.32, 184.09]
e_3	[33, 34, 28, 32]	[11.46, 15.27, 19.28, 19.29]	[0.00, 0.00, 0.00, 26.49]	[53.97, 65.68, 81.50, 100.71]
e_4	[47, 48]	[69.47, 268.22]	[0.00, 0.00]	[155.18, 594.79]
e_5	[5, 51, 6]	[3.82, 7.63, 53.13]	[0.00, 11.44, 0.00]	[38.17, 50.12, 334.34]
e_6	[52, 65, 66, 67, 9, 7,10, 11]	[7.63, 15.46, 25.47, 26.27, 45.16, 73.29, 94.79, 98.61]	[0.00, 0.00, 7.00, 1.94, 43.55, 56.17, 93.93, 97.86]	[46.32, 65.82, 75.39, 146.11, 198.41, 273.05, 303.82, 334.82]
e_7	[54, 53, 8, 58]	[15.47, 19.28, 64.59, 86.26]	[0.00, 1.19, 0.00, 0.00]	[71.47, 80.28, 170.15, 253.75]
e_8	[61, 64, 63, 60]	[29.78, 81.64, 169.46,952.47]	[0.00, 0.00, 0.00, 0.00]	[126.86, 228.32, 376.58, 1706.6]
e_9	[12, 13, 68, 15, 16, 17]	[7.64, 9.02, 33.92, 61.24, 81.63, 85.45]	[0.00, 0.00, 0.00, 0.00, 15.11, 39.04]	[50.66, 60.44, 112.28, 197.60, 241.97, 281.86]
e_{10}	[21, 19, 26, 25, 23, 20]	[7.63, 11.46, 16.65, 19.29, 22.45, 90.08]	[0.00, 0.00, 0.00, 10.86, 34.70, 0.00]	[76.64, 80.97, 124.41, 150.18, 156.93, 260.99]